Hydrobiologia (2018) 806:313–331
https://doi.org/10.1007/s10750-017-3371-4

PRIMARY RESEARCH PAPER

Reconsideration of the systematics of Peniculida (Protista, Ciliophora) based on SSU rRNA gene sequences and new morphological features of *Marituja* and *Dismatostoma*

Yuan Xu · Feng Gao · Xinpeng Fan

Received: 16 April 2017 / Revised: 29 August 2017 / Accepted: 30 August 2017 / Published online: 11 September 2017

Abstract Ciliated protists are unicellular eukaryotes that play important roles in aquatic ecosystems. One of the major tasks of ciliate taxonomy is to re-evaluate the systematic confusing taxa using modern methods. In the present study, two peniculid ciliates, *Marituja* cf. *caudata* and *Disematostoma minor* collected from east China, were studied using a multi-method approach. New morphological observations supplied additional information for species identification and systematic revision of the order Peniculida. The small subunit ribosomal RNA gene sequences of *M.* cf. *caudata*, *D. minor*, and *Frontonia terricola* were characterized for the first time and provided new insights into the phylogeny of Peniculida. The family Stokesiidae Roque, 1961, was expanded to include the genera *Disematostoma* and *Marituja* in addition to its type genus *Stokesia*, since the three genera formed a well-supported clade in the phylogenetic analyses. The diagnosis of Stokesiidae was improved to include the newly recognized synapomorphies, i.e., barren kinetosomes on the dorsal side, a ciliated dorsal suture, and the somatic ciliature that can be recognized as transversely oriented circles. Additionally, the systematic relationships of the genera and families of Peniculida were hypothesized. We argue that more diversified morphological features should be considered when assessing diagnostic traits for ciliate taxa during systematic revisions.

Keywords Ciliate · Frontoniidae · Maritujidae · Phylogeny · Stokesiidae · Taxonomy

Electronic supplementary material The online version of this article (doi:10.1007/s10750-017-3371-4) contains supplementary material, which is available to authorized users.

Handling editor: Diego Fontaneto

Y. Xu
State Key Laboratory of Estuarine and Coastal Research, East China Normal University, Shanghai 200062, China
e-mail: yxu@sklec.ecnu.edu.cn

F. Gao
Institute of Evolution and Marine Biodiversity, Ocean University of China, Qingdao 266003, China
e-mail: gaof@ouc.edu.cn

X. Fan (✉)
School of Life Sciences, East China Normal University, Shanghai 200241, China
e-mail: xpfan@bio.ecnu.edu.cn

Introduction

Ciliated protozoans are a group of unicellular eukaryotes that live in aquatic habitats where they are considered to be an important link in aquatic systems by feeding on small-sized particles and serving as readily assimilated prey for large zooplankton (Suzuki & Miyabe, 2007; Wiackowski & Kocerba-Soroka, 2017). The taxonomy of ciliates has relied on the observation of both living cells and prepared

specimens (Lynn, 2008; Warren et al., 2017). In recent decades, the analysis of gene sequences in addition to visualizing morphology has become a new recommendation for species description (Warren et al., 2017). Considering the methodologies for specimen preparation (e.g., silver staining methods, differential interference microscopy, and electron microscopy) were gradually established between 1920s and 1970s, and gene sequencing had not been used widely before 1990s, there are a considerable number of known species that have not been clearly documented and also some systematic confusion in taxa of different levels (Kahl, 1926, 1931; Corliss, 1979; Jankowski, 2007; Lynn, 2008). Therefore, conducting species redescription and reconsideration of systematic problems calls for the use of all currently available methodologies.

Ciliates in the order Peniculida Fauré-Frémiet in Corliss, 1956 are commonly found in fresh and marine waters. To date, more than 90 nominal species belonging to seven families and 14 genera have been reported, and molecular data covering six genera are available in the GenBank database (Lynn, 2008; Yildiz & Senler, 2013; Krenek et al., 2015). Current standards for identifying peniculids include the features of the buccal apparatus and somatic ciliature, characteristics of the contractile vacuole (its pores and collecting canals), and number and shape of the macronuclear nodules (Foissner et al., 1994; Foissner & Song, 2002; Long et al., 2005, 2008; Fokin et al., 2006; Fokin, 2008; Fan et al., 2011, 2013; Pan et al., 2013). Phylogenetic analyses using small subunit ribosomal RNA (SSU rRNA) gene sequences have contributed greatly in updating peniculid systematics (Strüder-Kypke et al., 2000; Gao et al., 2008; Fan et al., 2013; Gao et al., 2016). Recently, several other genes have been used to resolve inter- and intraspecies relationships of peniculids, and have confirmed the existence of cryptic species (Tarcz, 2013; Zhao et al., 2013, 2016; Krenek et al., 2015). However, species sampling remains unbalanced in these phylogenetic studies. Compared to the high number of identified specimens from *Frontonia* and *Paramecium*, there are relatively few representatives from other genera such as, *Marituja*, *Disematostoma*, *Clathrostoma*, and *Neobursaridium*. The bias in sampling can lead to uncertain assignment of taxa and impede further understanding of the evolutionary relationships among the families and genera within the order (Corliss, 1979; Strüder-Kypke et al., 2000; Fokin et al., 2006; Lynn, 2008; Fan et al., 2013; Zhao et al., 2016).

In the present study, two peniculids, *Marituja* cf. *caudata* and *Disematostoma minor*, were morphologically studied and the SSU rRNA gene of the two species and another peniculid, *Frontonia terricola,* were sequenced. The taxonomy of related families and genera were discussed, and the new systematic relationships among the members of Peniculida were also proposed.

Materials and methods

Sampling, observation, and identification

Marituja cf. *caudata* was collected on 9th June 2014 from a wetland area (31°35′02″N; 121°55′66″E) in Chongming Island, which is located in the estuary of Yangtze River, China. The high tidal region of the sampling site was covered with reeds, and the water salinity was about 2‰. *Disematostoma minor* was collected on 20th July 2014 from a fresh water puddle (29°48′16″N; 121°48′07″E) in Tiantong Mountain, Zhejiang Province, China. Specimens were collected by scooping water and sediment directly into a 500-ml jar. *Frontonia terricola* was collected from a natural farmland at Zulfi city, northwest of Riyadh, Saudi Arabia (26°22′01″N; 44°46′03″E). The soil sample was taken directly, and was then processed with the non-flooded Petri dish method in the laboratory (Foissner, 1987).

Cells were isolated using a micropipette, and observed in vivo using bright field and differential interference microscopy (Olympus BX51). The infraciliature and argyrome structures were revealed using the Chatton-Lwoff silver nitrate, silver carbonate, and protargol staining methods (Corliss, 1953; Wilbert, 1975; Ma et al., 2003), and measurements were made under ×100 to ×1250 magnification. Drawings were made with the help of a camera lucida. Samples for scanning electron microscopy (SEM) were prepared following the protocol of Gu & Ni (1993), and observed under a Hitachi S-4800 scanning electron microscope with accelerating voltage of 5.0 kV.

Taxonomic analyses of *Marituja* cf. *caudata* and *Disematostoma minor* were fully in line with recommendations proposed by Warren et al. (2017). *Frontonia terricola* was morphologically well documented

and our population corresponds well with the original description (Foissner, 1987). Therefore, we have only documented the diagnostic features below and in Fig. S1. Cells measured approximately 120 × 80 μm in vivo with a ratio of buccal field to body length of 30–40%. There were about 70 somatic kineties of body length and six postoral kineties arranged below the buccal field. Peniculi 1 and 2 were composed of four kinetidal rows, while peniculus 3 was three-rowed. Three vestibular kineties were on the right of the paroral membrane.

Terminology and systematics

Terminology and systematics are mainly according to Lynn (2008). Some peniculid-restricted terms are explained as follows and illustrated in Fig. 1.

Nematodesmata birefringent bundle of parallel microtubules, kinetosome-associated; plunging into the cytoplasm at right angles to the pellicle, and arranged in oral and/or postoral areas of peniculids.

Preoral suture typically, a short, midventral line or secant system extending often to the left, from the oral region to the apical pole of the organism and onto which the anterior ends of a number of somatic kineties from either side may converge.

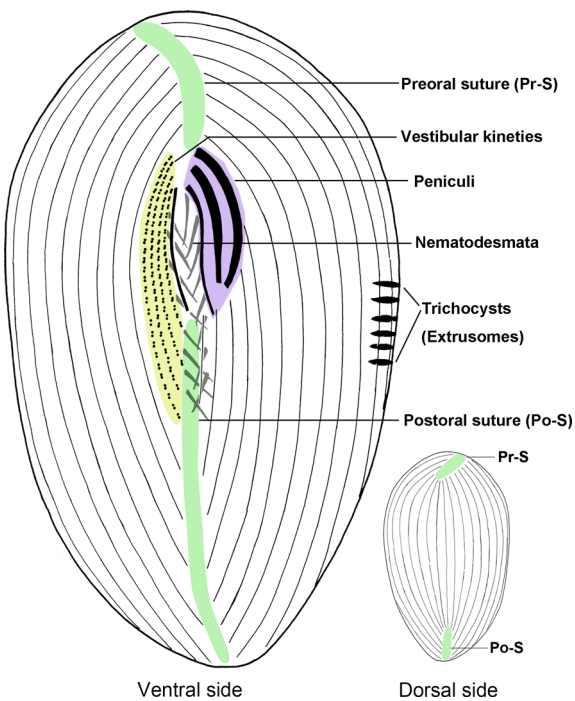

Fig. 1 Illustration of some peniculid-restricted features

Peniculi a type of oral polykinetid in the form of a long band of often short, seemingly fused cilia; its infraciliary base, typically coursing along the left wall of a buccal cavity, may be as many as 11 kinetosomes in width but is usually only 3–7, with tapering to still lower numbers at either end.

Vestibular kineties Three or more somatic kineties, often with dikinetids (the kinetids composed of two kinetosomes and their fibrillar associates) and single associated parasomal sac forming a triangular group as revealed in silver-impregnated material; on the ventral surface near the anterior end of the body and located immediately to the right of the buccal cavity; may represent a legitimate part of the buccal ciliature sensu lato.

Postoral suture typically, a midventral secant system or line coursing from the oral region toward the posterior pole of the organism and onto which the posterior extremities from both sides converge or run roughly parallel to it.

Extrusomes a generalized term used to refer to various types of probably non-homologous membrane-bounded organelles; extrusion occurs under conditions of appropriate chemical or mechanical stimulation.

Trichocysts spindle-shaped, non-toxic, explosive extrusomes; in the mature stage, consisting of an apical tip, shaped like an inverted golf tee, and a long, fusiform, fibrous shaft; on ejection, following an appropriate stimulus, acquiring a characteristic periodic structure; their function is often defensive.

DNA extraction, PCR amplification, and sequencing

Genomic DNA extraction, PCR amplification, and sequencing of the SSU rRNA gene were performed according to the method of Huang et al. (2014). Genomic DNA was extracted from cleaned cells using the DNeasy Tissue kit (Qiagen, CA), and the SSU rRNA gene was amplified using Q5® Hot Start High-Fidelity DNA Polymerase (NEW ENGLAND BioLabs, USA) with the primers: 18 s-F (5′-AAC CTG GTT GAT CCT GCC AGT-3′) and 18s-R (5′-TGA TCC TTC TGC AGG TTC ACC TAC-3′) (Medlin et al., 1988). PCR products were sequenced directly or were inserted into the pEASY-T1 vector (TransGen Biotech, Beijing, China) and transformed into competent cells. Sequencing was performed bidirectionally on an ABI 3700 sequencer (GENEWIZ Biotechnology Co., Ltd., Beijing, China).

Phylogenetic analyses

In addition to the three newly obtained SSU rRNA gene sequences, the sequences of another 100 closely related species/populations were obtained from the NCBI GenBank database and used in the present analyses. Four prostomateans were chosen as the outgroup species. Sequences were aligned using the GUIDANCE algorithm (Penn et al., 2010b) with default parameters in the GUIDANCE web server (Penn et al., 2010a). The final alignment including 1786 nucleotides and 103 taxa was used for phylogenetic analyses (available from the authors upon request).

Maximum likelihood (ML) analysis was performed with RAxML-HPC2 on XSEDE v.8.2.4 (Stamatakis, 2014) on the CIPRES Science Gateway (Miller et al., 2010) using the GTR + I + G model as the optional choice selected by Modeltest v.3.4 (Posada & Crandall, 1998). Support for the best-scoring ML tree came from 1000 bootstrap replicates. Bayesian inference (BI) analysis was performed with MrBayes on XSEDE v.3.2.6 (Ronquist & Huelsenbeck, 2003) on the CIPRES Science Gateway using the GTR + I + G evolutionary model as the best-fit model selected by MrModeltest v.2 (Nylander, 2004). Markov chain Monte Carlo (MCMC) simulations were run with two sets of four chains for 10,000,000 generations, with a sample frequency of 100 generations. After discarding the first 10,000 trees as burn in, all the remaining trees were used to calculate the posterior probability using a majority rule consensus. SeaView v.4 was used to visualize tree topology (Gouy et al., 2010).

Results

Order Peniculida Fauré-Frémiet in Corliss, 1956

Family Stokesiidae Roque, 1961
Marituja cf. *caudata* Obolkina (1995) (Figs. 2, 3, 4, and 5; Table 1)

Description of the isolated organism

Cells in vivo were 115 to 160 × 70 to 90 μm in size and conically shaped in outline. The buccal opening was conspicuous and measured about 60 × 30 μm (Figs. 2A; 3A–C, E–H). When viewed laterally, the buccal field margin was oblique to the longitudinal axis; the buccal cavity was deepest in the anterior third, and almost reached the dorsal side (Fig. 3C, F). The nematodesmata associated with the peniculi were about 30 μm long (Figs. 3M, 5D). Cells prepared for SEM were oval in shape; the buccal opening had an "S"-shaped right margin and a tick-like left margin (Fig. 4A–C, K, L). Cells were moderately flexible, which resulted in variable location and shape of the buccal field (Fig. 4A–C). A large number of food vacuoles existed in the cytoplasm, and there were yellow- or brown-colored algae in some of the food vacuoles (Fig. 3A–D). The contractile vacuole was near equatorial line of the cell and near the right margin and dorsal side, and measured about 25 μm across when they were fully extended (Figs. 2A, 3D). There were about six associated collecting canals which can be observed only when the cells were compressed (Fig. 3J). The contractile vacuole had one or two pores on the dorsal side (Fig. 4E, I). The macronucleus was elongated and distinctly curved, occupying most of the body length (Figs. 2F, 5C). The fusiform-shaped trichocysts were located beneath the pellicle and 8–9 μm long (Fig. 3I); extruded structures were about 20 μm and had curved tips (Fig. 4B, H).

There were 118–145 somatic kineties (including 18 postoral kineties), which contained monokinetids near the posterior end and dikinetids on the rest of the cell (Figs. 2B, C, E, 5A, B, J). The postoral kineties began behind the buccal field, and were shortened in length from the left to the right (Figs. 2D, 5H). The kinetids of the somatic kineties were arranged in horizontal circles in most of the cell, but oriented obliquely at the ventral right of the oral field (Figs. 2B, C, 5A, B). Somatic cilia were 10–13 μm long. Somatic kineties ran down both of the ventral and dorsal sides, resulting in three sutures: preoral suture, postoral suture, and dorsal polar band (DPB, see Discussion for term explanation) (Figs. 2B, C, E, 3G, K, 4E–G, I, J, 5I). The preoral suture was short and extended towards the anterior pole; the postoral suture was long and straight (Figs. 2B, C, 5I). Under SEM, some dikinetids in the first kinetidal circle that surround the preoral suture were possibly unciliated (Fig. 4F, G). The dorsal polar band was obliquely oriented and occupied 40% of the body length; it terminated posteriorly near the caudal end connecting with the postoral suture, and terminated anteriorly close to the contractile vacuole pore

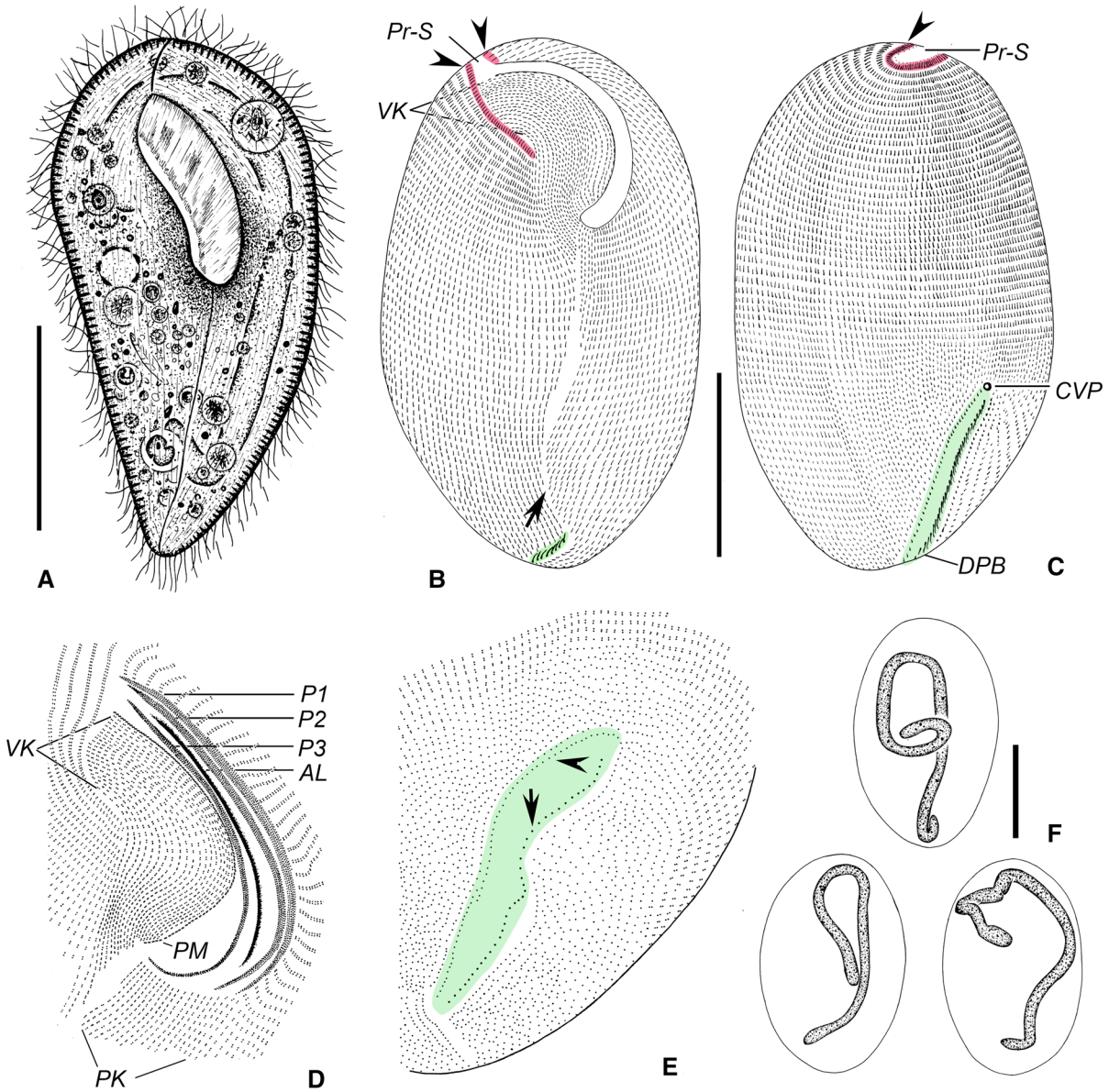

Fig. 2 **A–F** Morphology of *Marituja* cf. *caudata* from life (**A**), after staining with silver carbonate (**B**, **C**) and protargol (**D–F**). **A** Ventral view of a representative individual. **B** and **C** Ventral (**B**) and dorsal **C** views of infraciliature (peniculi are not shown) and dorsal polar band, especially showing the preoral suture (Pr-S), postoral suture (*arrow*), vestibular kineties (VK), the first kinetidal circle that surrounds the preoral suture (*arrowheads*), dorsal polar band (DPB), and the contractile vacuole pore (CVP). **D** Details of the buccal apparatus. **E** Dorsal-posterior of cell, showing the posterior body containing monokinetids, *arrowhead* and *arrow mark* the left and right row of DPB, respectively. **F** Different macronucleus shapes in three individuals. *AL* argentophilic line; *CVP* contractile vacuole pore; *DPB* dorsal polar band; *P1, 2, 3* peniculi 1, 2, and 3; *PM* paroral membrane; *Pr-S* preoral suture; *VK* vestibular kineties; *PK* postoral kineties. *Scale bars* 50 μm

(Figs. 2B, C, 4E, I, J, 5B). The dorsal polar band contained two rows of heavily stained kinetosomes; the kinetids in the right row were associated with conspicuous fibers (Figs. 2C, E, 5B). The kinetosomes of the kinetidal rows of the dorsal polar band were ciliated (with cilia about 16 μm long); while the other kinetosomes around the dorsal polar band were barren (Figs. 3K, 4E, I, J).

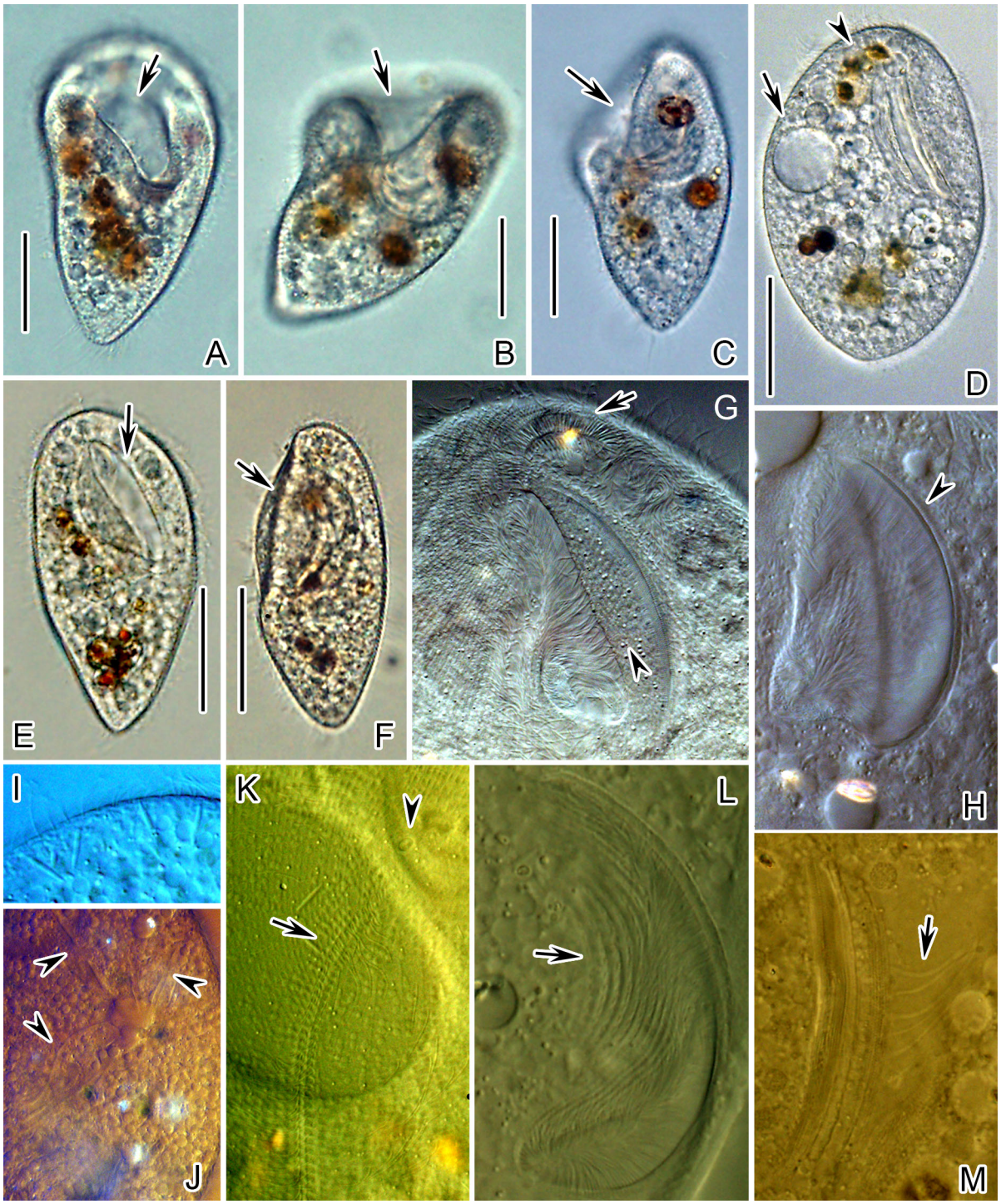

The oral apparatus was as shown in Figs. 2D, 5D–G. The peniculi (P) 1 and 2 were located close together. P1 and P2 had six and five kinetidal rows, respectively; the left-most outer row of the two peniculi was shortened from both ends; P3 was four-rowed with its posterior part distinctly curved

◀**Fig. 3** **A**–**M** Photomicrographs of *Marituja* cf. *caudata* from life. **A**–**C** Same individual from different angles, showing the general body shape and the large deepened buccal cavity (*arrow*). **D** Slightly compressed individual, showing the food vacuoles (*arrowhead*) and the contractile vacuole (*arrow*). **E** and **F** Ventral (**E**) and lateral (**F**) view of the same individual showing the body shape and the buccal cavity (*arrow*). **G**, **H**, and **L** Details of buccal portion, showing the preoral suture (*arrow* in **G**), the lip (*arrowhead* in **G**) on the left of buccal area that covers the peniculi (*arrowhead* in **H**), and vestibular kineties (*arrow* in **L**). **I** Resting trichocysts in the pellicle. **J** Collecting canals (*arrowheads*), which were only observed when the cell was severely compressed. **K** Dorsal-posterior view of cell, showing the dorsal polar band (*arrow*), the contractile vacuole pore (*arrowhead*), and the unciliated area near dorsal polar band. **M** The nematodesmata (*arrow*) associated with the peniculi. *Scale bars* 50 μm

(Figs. 2D, 5E–G). The paroral membrane was possibly composed of dikinetids (Figs. 2D, 5D) and there were 16–21 gently curved vestibular kineties that were composed of dikinetids (Figs. 2D, 3L, 5D). Under SEM, the oral apparatus was observed to be located at the inner wall of the cavity, and the cilia of the peniculi were approximately 25 μm long (Fig. 4F, K, L).

Cells swim moderately fast and rotate around the longitudinal axis whilst pivoting at the posterior end causing cells to swing from side to side as they move forwards.

Remarks

The genus *Marituja* comprises only two species, *M. pelagica* and *M. caudata*. The type species, *M. pelagica*, has a stubby-shaped body, 104–127 somatic kineties and 9–14 vestibular kineties; peniculi 1, 2, and 3 have three, four, and four kinetosome rows, respectively (Wilbert, 1972; Packroff & Wilbert, 1991). Our isolate cannot be conspecific with *M. pelagica* because of the differences in body shape and number of kinetal rows in the peniculi. *M. caudata* was described only once in an original report based on the population from Baikal (Obolkina, 1995). Our isolate shares similarities with the Baikal population of *M. caudata* in terms of body size, pointed caudal end, and the buccal cavity at a certain angle to the main body axis, but differs in having more somatic kineties (118–145 vs. 100–110) and vestibular kineties (16–21 vs. 6–8). Additionally, they differ in the composition of peniculi 1–3: peniculi 1, 2, and 3 comprising four, four, and three rows, respectively, in the Baikal isolate, and six, five, and five rows, respectively, in the Chinese isolate. It has to be mentioned that the original report did not provide clear illustrations of the kinetidal rows of peniculi, and the specimen preparation appears to be poorly conducted judging from the protargol staining pictures. There may be errors in the kinetidal row counts that were reported in the original description. Moreover, the number of the vestibular kineties is uncertain and needs to be restudied (personal communication with Dr. Olbolkina). Therefore, we identified our isolate as *M.* cf. *caudata*, until further data about the Baikal population are available to avoid synonyms.

Disematostoma minor Kahl, 1931 (Figs. 6, 7; Table 2)

Description of the isolated organism

Cells in vivo were 85 to 90 × 60 to 70 μm in size; the body was oval with an inconspicuous tapered caudal end (Figs. 6A, 7A, B); well-fed cells were irregularly spherical (Fig. 7B). Cells prepared for SEM were inverted cone shaped (Fig. 7D, E). The buccal field occupied 25% of the body length; its left and right margins were convex (Fig. 6A, D). The cytoplasm contained a large number of food vacuoles with ingested flagellates (Fig. 6A). The contractile vacuole was in the right half of equatorial line and near the dorsal side with about eight collecting canals (Figs. 6A, 7C) and a single pore (Fig. 7E, M). The sausage-like macronucleus was near the anterior half and usually curved to the left in a "C" shape (Figs. 6C, E, 7L). The resting trichocysts were 6–7 μm long in living cells (Fig. 6A), and the extruded structures were about 13 μm in SEM prepared samples (Fig. 7D).

Cells swim fast while rotating around the caudal end, and the movement looks like the locomotion of *Marituja* cf. *caudata*.

There were 80–87 somatic kineties (including 6–8 postoral kineties) that were a mixture of dikinetids and monokinetids. On the ventral side, only a small area near the rear end was covered by monokinetids (Fig. 6D), while the dorsal side contained monokinetids occupying the posterior half (Figs. 6E, 7L). The kinetosomes of somatic kineties can be recognized as 21–25 transverse kinetidal circles, including those near the oral field which are more obliquely oriented (Figs. 6D, E, 7F, G). Somatic cilia were 8–10 μm long. The preoral suture extended to the anterior pole

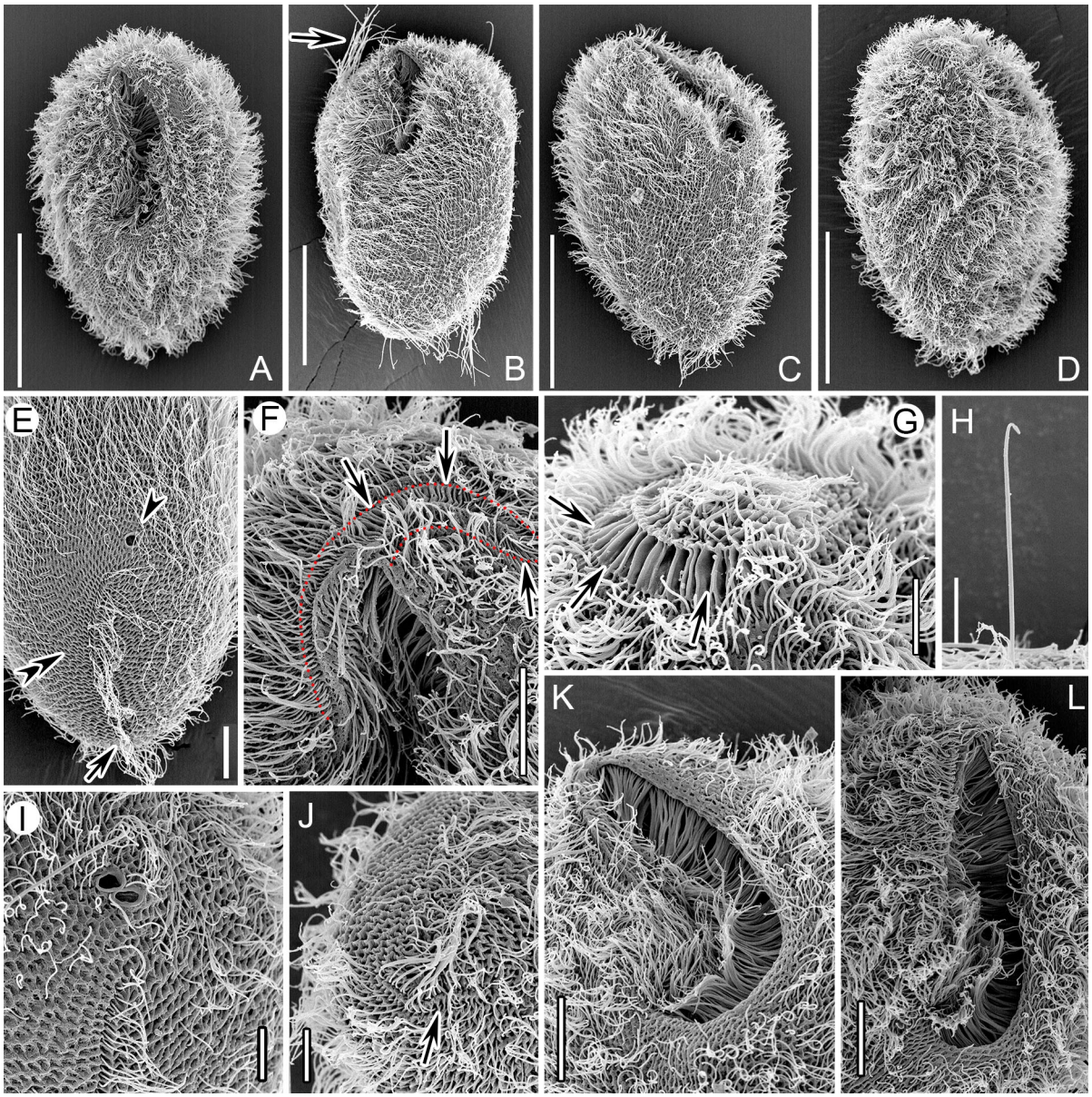

Fig. 4 **A–L** Scanning electron micrographs of *Marituja* cf. *caudata*. **A–D** Ventral (**A**, **B**) and lateral view (**C**, **D**) of different individuals, showing the general morphology, especially the body shape and location of the buccal opening. An *arrow* indicates the extruded trichocysts. **E** Dorsal view of an individual showing the unciliated area (*double-arrowhead*), the dorsal polar band (*arrow*), and the single contractile vacuole pore (*arrowhead*). **F** and **G** Anterior portion (**F**) and apical end (**G**) where arrows point to the first kinetidal row (*dashed line* in **F**) that are partly unciliated. **H** Ejected structure of trichocysts. **I** Dorsal view of an individual that has two contractile vacuole pores. **J** Antapical view showing the posterior end of dorsal polar band (*arrow*). **K** and **L** The curved buccal margins and peniculus 1 (*arrow*), and **L** the less curved buccal margin in another individual. *Scale bars* 40 µm (**A–D**); 5 µm (**G–J**); 10 µm (**E**, **F**, **K**, **L**)

and were surrounded by the first transverse kinetidal circle that were partially barren of cilia (Figs. 6D, 7D, G). The postoral suture intersected transverse circles behind the oral field (Figs. 6D, 7F). The dorsal polar band occupied half of the body length with cilia which were about 13 µm long; the right row comprised about 20 monokinetids associated with heavily stained fibers that were arranged more loosely than those in the left

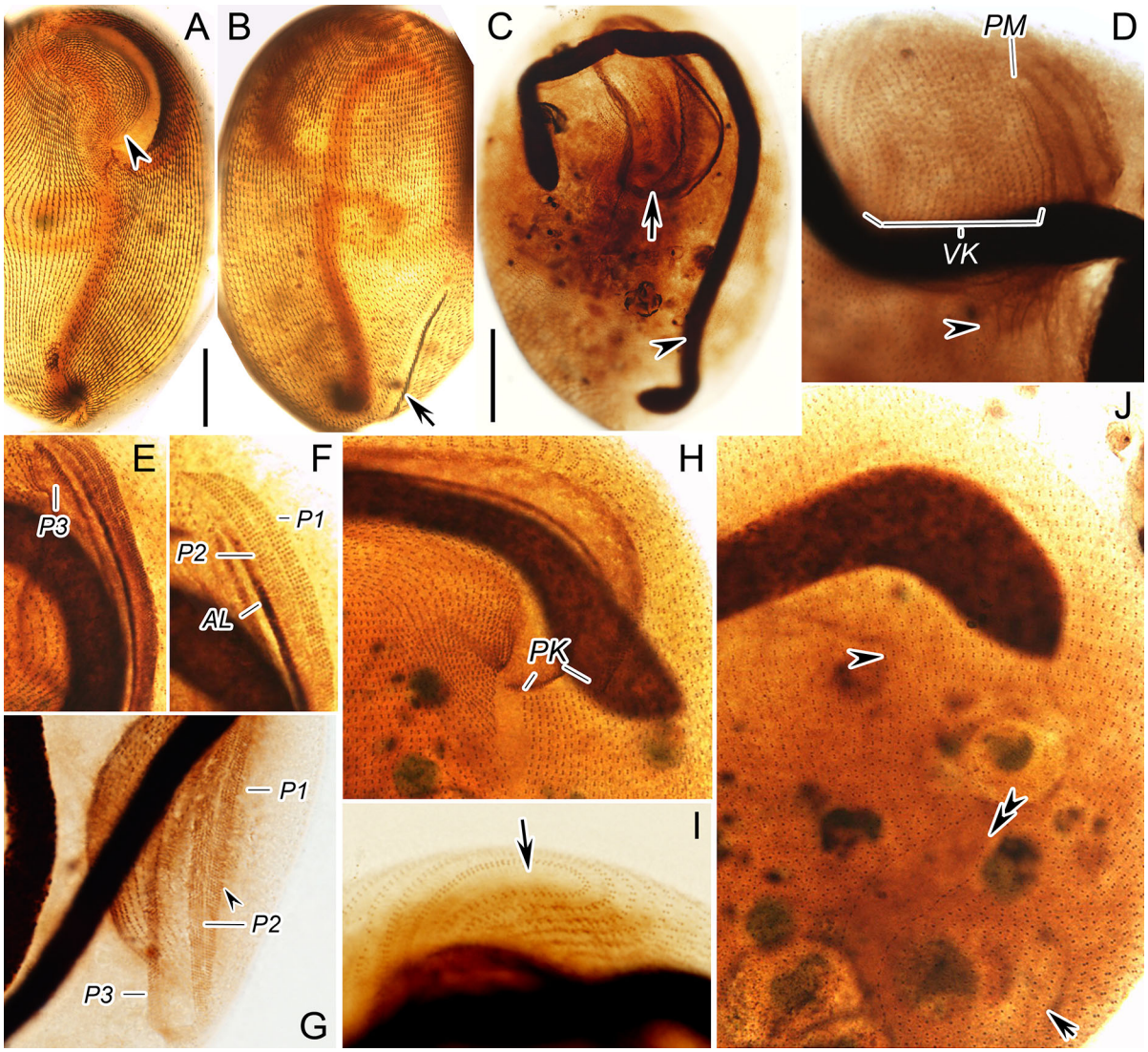

Fig. 5 **A–J** *Marituja* cf. *caudata* stained with silver carbonate (**A**, **B**) and protargol (**C–J**). **A** and **B** Ventral (**A**) and dorsal (**B**) view of the same individual showing the general infraciliature, where arrowhead marks the vestibular kineties, and the arrow indicates the dorsal polar band. **C** The general view of the buccal apparatus (*arrow*) and macronucleus (*arrowhead*). **D** The paroral membrane and vestibular kineties, and the *arrowhead* refers to the nematodesmata associated with peniculi. **E–G** Details of the buccal apparatus, showing peniculi 1, 2, 3, and the argentophilic line, and the *arrowhead* in (**G**) marks the left outer row of the six-rowed peniculus 1. H, I. The postoral kineties (PK) and the preoral suture (*arrow* in **I**) surrounded by the first transverse kinetidal circle. **J** The dorsal side of an individual, showing the dikinetids at the anterior (*arrowhead*) and monokinetids at the posterior of the cell (*arrow*), and the right kinetidal row of dorsal polar band (*double-arrowhead*). *AL* argentophilic line; *P1, 2, 3* peniculi 1, 2, and 3; *PM* paroral membrane; *VK* vestibular kineties; *PK* postoral kineties. *Scale bars* 20 μm (**A**); 30 μm (**C**)

row (Figs. 6E, 7H, L). The kinetosomes in the posterior half were unciliated except for those in the dorsal polar band (Fig. 7E, M).

Oral apparatus is shown in Figs. 6B, 7I–K. P1 was composed of three kinetosome rows, while P2 was five-rowed; the rows in P1 and P2 decreased in kinetosome numbers from left to right; P3 comprised four equal rows, and was curved in a "S" shape (Figs. 6B, 7I, J). The paroral membrane comprised densely arranged dikinetids; there were six vestibular kineties at right of the paroral membrane, composed of evenly distributed dikinetids (Figs. 6B, 7K).

Table 1 Morphometric characteristics of *Marituja* cf. *caudata* from specimens after silver staining

Characters	Min	Max	Mean	SD	CV	N
Body length in μm	98	140	120.9	12.9	10.7	15
Body width in μm	55	100	80.3	17.4	21.7	14
Ratio of BF/BL (in %)	34*	50*	43.9*	4.7	10.6	15
Somatic kineties, number	118	145	132.8	10.0	7.6	8
Vestibular kineties, number	16	21	18.3	1.7	9.5	11
Macronucleus, length	95	220	176.4	35.7	20.2	10

The asterisk (*) indicates data using the Chatton-Lwoff silver nitrate staining method, and other data were collected after Wilbert's protargol staining

CV coefficient of variation in %; *Max* maximum; *Mean* arithmetic mean; *Min* minimum; *N* number of specimens investigated; *SD* standard deviation of the mean

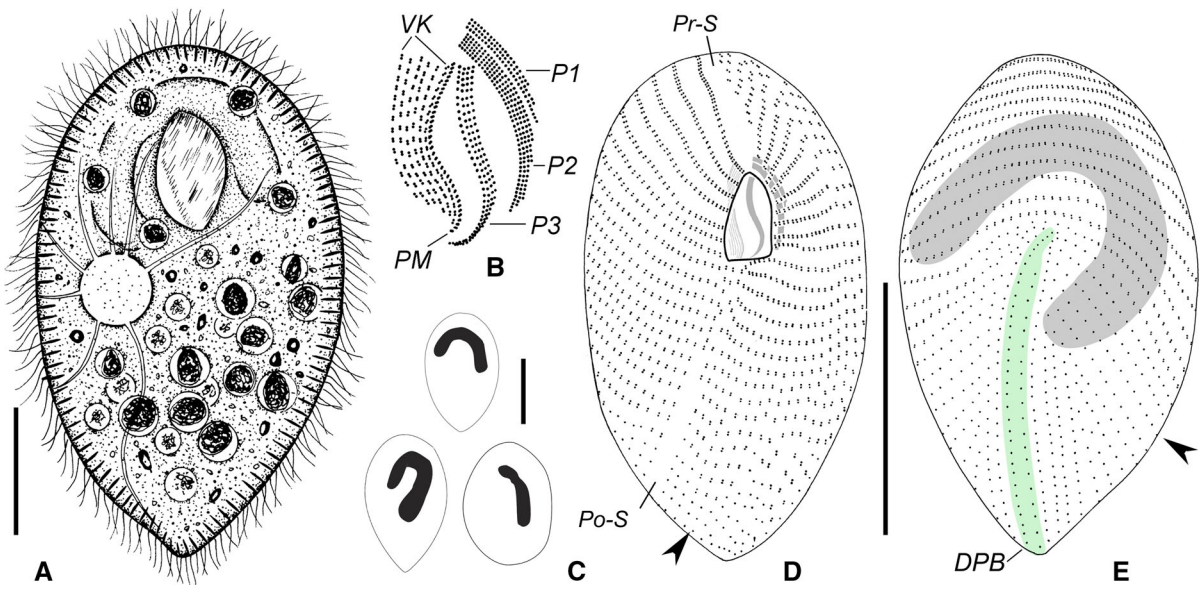

Fig. 6 **A**–**E** Morphology of *Disematostoma minor* from life (**A**) and after protargol staining (**B**–**E**). **A** Ventral view of a typical individual. **B** Detailed ciliature of the buccal apparatus. **C** The different shape of macronucleus. **D** and **E** Ventral and dorsal view of general ciliary patterns, the preoral suture (Pr-S), postoral suture (Po-S) and the monokinetid in the posterior on both sides (*arrows*). *DPB* dorsal polar band; *P1, 2, 3* peniculi 1, 2, and 3; *PM* paroral membrane; Pr-s, preoral suture; Po-S, postoral suture; *VK* vestibular kineties. *Scale bars* 20 μm (**A**); 40 μm (**C**, **D**, **E**)

Remarks

This species was originally described as *D. butschlii* var. *minor* by Kahl (1926), and subsequently identified as a separate species, *D. minor* by Kahl (1931). Michiels & Wilbert (1973) redescribed it and updated the information on general morphology and details of the oral apparatus. The present population is consistent with previous reports in having an oval body shape, and the same number of vestibular kineties and kinetidal rows in peniculi 1 and 3. Additionally, all three populations have relatively smaller body size in vivo (<100 μm in length) compared to other *Disematostoma* species (Tuffrau & Savoie, 1961; Martin-Gonzaleaz et al., 1990), though they differ slightly from each other (85 to 90 × 65 to 70 μm in the present population, 50 to 60 × 31 to 37 μm in Kahl's population and 78 × 57 μm in Michiels & Wilbert's population). The evident differences lie in the number of somatic kineties (81 in the present

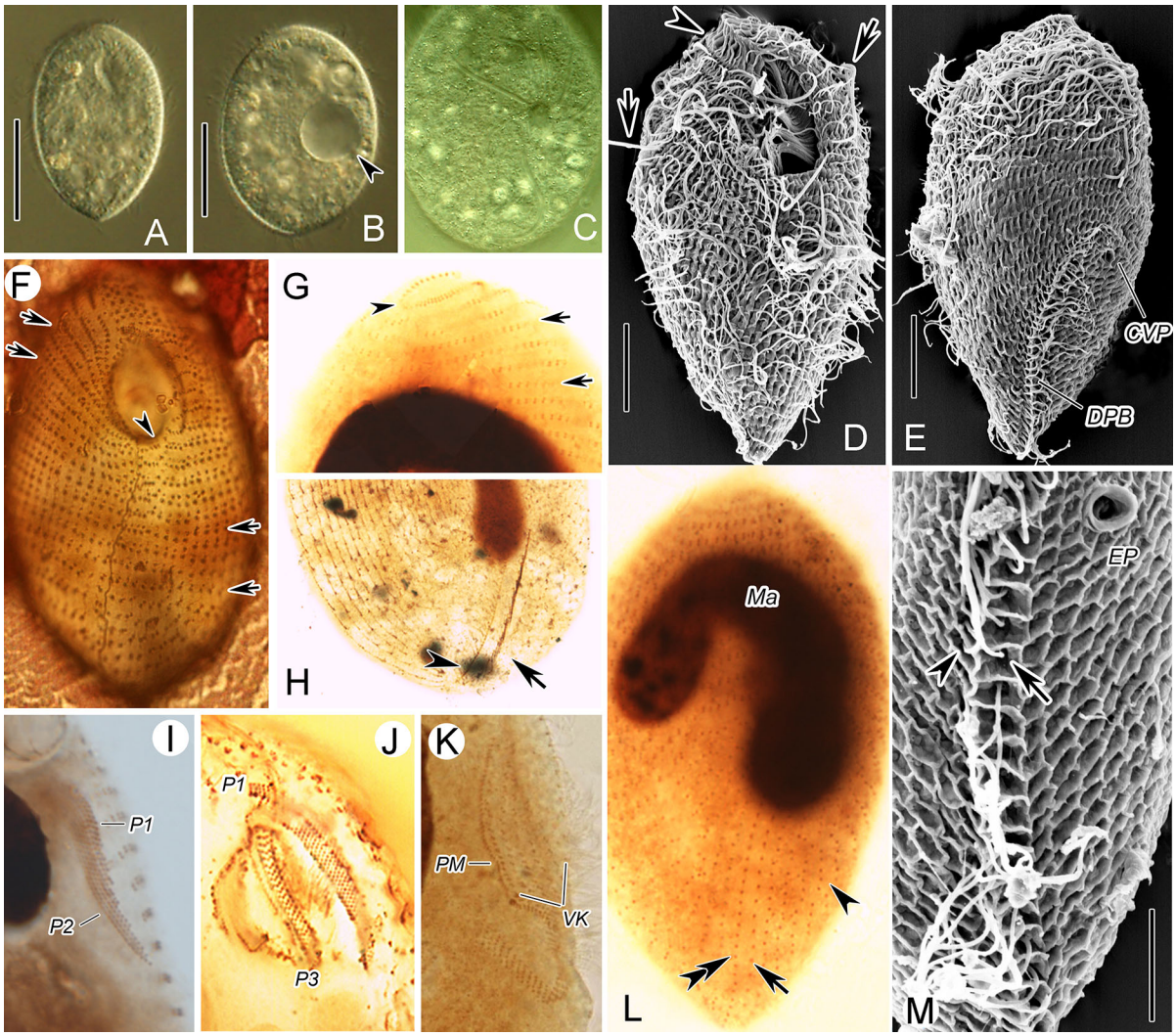

Fig. 7 **A**–**M** Micrographs of *Disematostoma minor* from life (**A**–**C**), under scanning electron microscopy (**D**, **E**, **M**), and after staining with silver nitrate (**F**, **J**), silver carbonate (**H**), and protargol (**G**, **I**–**L**). **A** and **B** Ventral (**A**) and dorsal (**B**) views of typical individuals, showing body shape and contractile vacuole (*arrowhead* in **B**). **C** Dorsal view of a slightly compressed individual showing the collecting canals. **D** and **E** Ventral (**D**) and dorsal (**E**) views of *Disematostoma minor*, showing the buccal opening, preoral suture (*arrowhead* in **D**), extruded structure of trichocysts (*arrows* in **D**) and dorsal polar band (DPB). **F** Ventral view showing the transversely or obliquely oriented somatic ciliature (*arrows*), and the postoral kineties (*arrow*). **G** Dorsal–anterior view, showing the first transverse kinetidal circle that surrounds the preoral suture (*arrowhead*) and somatic ciliature made of dikinetids in the anterior (*arrows*). **H** The dorsal polar band, where the *arrow* indicates the right row that is associated with stronger fibers, and the *arrowhead* marks the left row. **I**–**K**. Details of the buccal ciliature showing the peniculi 1, 2, and 3 (P1, 2 and 3), vestibular kineties (VK) and paroral membrane (PM). **L** Dorsal view showing the monokinetids in the posterior half (*arrowhead*), and the left (*double-arrowheads*) and right (*arrow*) kinetidal rows of the dorsal polar band. **M** Posterior part of dorsal side showing the unciliated area around the dorsal polar band, and the contractile vacuole pore (CVP), where arrow and arrowhead mark the right and left row of dorsal polar band, respectively. *DPB* dorsal polar band; *CVP* contractile vacuole pore; *P1, 2, 3* peniculi 1, 2, and 3; *PM* paroral membrane; *Ma* macronucleus; *VK* vestibular kineties. *Scale bars* 40 μm (**A**, **B**); 10 μm (**D**, **E**); 5 μm (**M**)

population vs. 72 in Michiels and Wilbert's population, on average) and kinetidal rows in peniculus 2 (five in the present population vs. four in Michiels and Wilbert's population). However, we consider these are population-dependent variations, and the measurement of kinetidal rows of peniculus 2 might even be an

Table 2 Morphometric characteristics of *Disematostoma minor* from specimens after silver staining

Characters	Min	Max	Mean	SD	CV	N
Body length in μm	69	94	80.6	6.5	8.1	25
Body width in μm	41	59	47.9	4.5	9.4	25
Ratio of BF/BL (in %)	21*	29*	23.9*	2.0	8.5	15
Somatic kineties, number	80	87	83.7	3.5	4.2	3
Vestibular kineties, number	6	6	6.0	0	0	4
Macronucleus, length	21	63	47.8	9.8	20.6	25

The asterisk (*) indicates data using the Chatton-Lwoff silver nitrate staining method, and other data were collected after Wilbert's protargol staining

CV coefficient of variation in %; *Max* maximum; *Mean* arithmetic mean; *Min* minimum; *N* number of specimens investigated; *SD* standard deviation of the mean

error since the outer row is not always recognizable in poorly stained specimens.

SSU rRNA gene-based phylogeny of Peniculida (Fig. 8)

The newly characterized SSU rRNA gene sequences have been deposited in GenBank with the length, GC content, and accession numbers as follows: *Marituja* cf. *caudata*—1701 bp, 45.33%, MF926594; *Disematostoma minor*—1693 bp, 45.36%, MF926592, *Frontonia terricola*—1701 bp, 45.44% MF926593.

The topologies of the ML and BI trees were concordant; therefore, the single topology of the BI tree is presented with support values from both algorithms on branches (Fig. 8). The six subclasses in Oligohymenophorea, Hymenostomatia, and Peritrichia formed a highly supported clade (95% ML, 1.00 BI), while Scuticociliatia, Apostomatia, and Astomatia grouped together (68% ML, 0.76 BI). Within the subclass Peniculia, the order Peniculida was sister to all the other oligohymenophoreans, while the order Urocentrida clustered with the Hymenostomatia and Peritrichia clade (85% ML, 1.00 BI). The phylogenetic tree included 38 species/isolates of Peniculida representing seven genera and five families. Lembadionidae was sister to the other peniculids that were included in the phylogenetic analysis. The genera *Disematostoma*, *Marituja*, and *Stokesia* formed a fully supported clade. Within this clade, *Disematostoma minor* clustered with the two *Marituja* species (99% ML, 1.00 BI), while the other two unidentified *Disematostoma* species formed a group with *Stokesia vernalis* (97% ML, 0.98 BI). *Frontonia* species were distributed into three clades. First, the newly characterized *Frontonia terricola* formed a fully supported clade with the genera *Disematostoma*, *Marituja*, and *Stokesia*. The second clade contained *Frontonia* sp. (FN667825), *F. ocularis*, *F. pusilla*, *F. elegans*, and *F. didieri* first clustered with *Apofrontonia*, which then grouped with *Paramecium* with full support. Lastly, the other 12 *Frontonia* species grouped together with full support. Based on the phylogenetic analyses, we noted that the *Stokesia* sp. (GenBank accession number KJ475264) was misidentified by Zhao et al. (2013). After considering the limited morphological data provided by the authors (personal communication with the authors), the isolate (KJ475264) has the typical ciliature of *Marituja*, and the identity of this isolate was thus corrected to *Marituja* sp.

Discussion

Remarks on dorsal polar band and suture of peniculids

The dorsal polar band is a dorsal suture that starts from the area near the mid-body and extends to the posterior pole in *Marituja* and *Disematostoma*; compared with the preoral and postoral suture, the dorsal polar band is characterized by having two ciliated kinetidal rows and more developed associated fibers for the right row

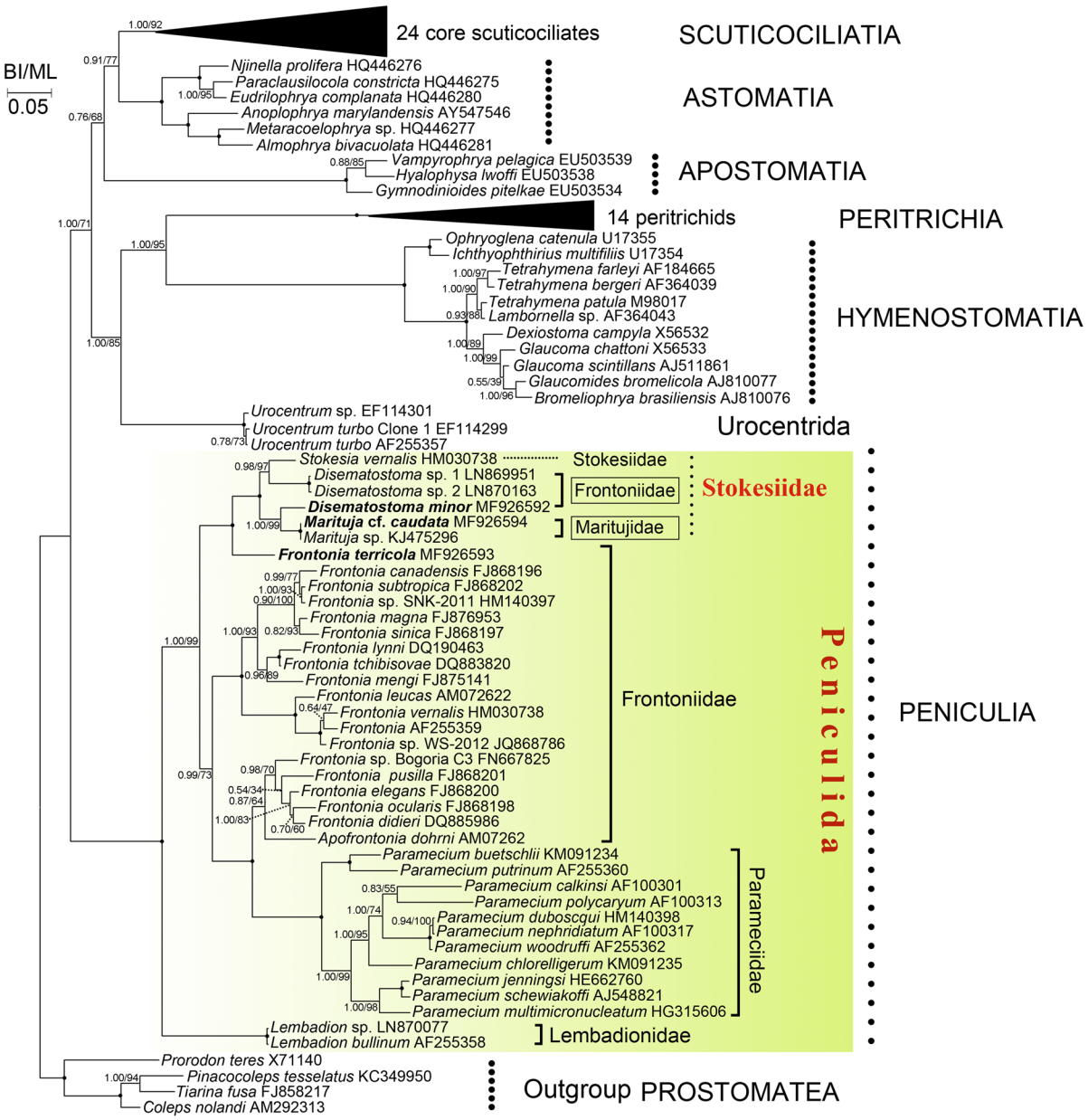

Fig. 8 Bayesian inference tree based on SSU rRNA genes focusing on Peniculida species. Positions of *Marituja* cf. *caudata*, *Disematostoma minor*, and *Frontonia terricola* are highlighted in *bold*. *Prorodon teres*, *Pinacocoleps tesselatus*, *Tiarina fusa*, and *Coleps nolandi* are the outgroup taxa. Taxa in *rectangles* (Frontoniidae and Maritujidae) show the previous familial arrangement of relative genera. *Numbers near nodes* are bootstrap values for Bayesian inference and the posterior probabilities for maximum likelihood, respectively. Accession numbers are listed after each species name. *Black circles* indicate the fully supported nodes in both analyses. The *scale bar* corresponds to 0.05 expected substitutions per site

(Serrano et al., 1990, 1994; Krainer, 1988; Packroff & Wilbert, 1991). Additionally, a considerable area around the dorsal polar band is unciliated. The dorsal suture of *Stokesia* as shown in Foissner et al. (1999) is also ciliated, and is thus similar to the dorsal polar band; however, it is essentially the preoral suture that extends over the dorsal side and does not reach the rear end (Foissner et al., 1994, 1999).

Our SEM observations of *M.* cf. *caudata* and *D. minor* show that some of the dikinetids in the first

kinetal circle around the preoral suture are possibly unciliated. This phenomenon was also observed in the SEM images of *Frontonia leucas* in Foissner et al. (1994). We infer that this may be a common feature shared by the three genera that was not noticed previously. Another possibility is that the kinetids of this area can be deciliated more easily during SEM preparation.

The systematic positions of *Marituja, Dissematostoma,* and *Frontonia*

Marituja Gajewskaja, 1928, was assigned to Stokesiidae by Corliss (1979), but was considered as a separate family (Maritujidae) by Jankowski in Small & Lynn (1985) and Lynn (2008). *Disematostoma* Lauterborn, 1894, was widely accepted as a member of Frontoniidae, while *Stokesia* was the type genus of the monotypic family Stokesiidae Roque, 1961 (Corliss, 1979; Jankowski, 2007; Lynn, 2008). In our phylogenetic analyses, *Marituja*, *Disematostoma*, and *Stokesia* formed a monophyletic group in a fully supported clade, indicating their close evolutionary relationship. Both *Marituja* and *Disematostoma* have an unciliated area on the dorsal side and a ciliated dorsal suture (i.e., dorsal polar band). These features coincide with the description of dorsal ciliature in *Stokesia* where the authors noted, "the dorsal side is barren, except for the suture" (Foissner et al., 1999). Moreover, *Disematostoma* and *Stokesia* also have somatic cilia arranged in distinct transverse paratenes, a diagnostic feature of *Marituja* (Small & Lynn, 1985; Serrano et al., 1990; Packroff & Wilbert, 1991). Considering their close affiliation revealed by phylogenetic analyses and their newly recognized morphological similarities, we therefore transfer *Disematostoma* into the family Stokesiidae, and support the assignment of *Marituja* to Stokesiidae, as suggested by Corliss (1979). Based on ICZN (1999), Maritujidae Jankowski in Small & Lynn (1985), is thus a junior synonym. The diagnosis for Stokesiidae was improved to include the newly summarized characteristics: body distinctively cone- or heart-shaped; somatic cilia forming transverse or obliquely oriented lines; part of dorsal side barren of cilia; bearing a ciliated dorsal suture; oral conspicuous, with few to many vestibular kineties; fresh-water habitat, planktonic. We argue that the systematic revisions of ciliated protozoans can only be convincing when considering the support of both molecular and morphological data, and we also argue that more diversified morphological features should be evaluated during the identification diagnostic traits of taxa.

Within the newly refined family Stokesiidae, *Disematostoma* is close to *Marituja* and they share the dorsal polar band which is lacking in *Stokesia* (Martin-Gonzaleaz et al., 1990; Serrano et al., 1990; Packroff & Wilbert, 1991; Obolkina, 1995; Foissner et al., 1999). However, in the topology of the present trees, *Disematostoma* was paraphyletic and two unidentified *Disematostoma* species (LN869951 and LN870163) clustered with *Stokesia*. We speculate that the identity of the two sequences might be incorrect, since the morphological data were well presented (personal communication with Dr. Fokin). If represented by *Disematostoma minor*, *Disematostoma* clustered with *Marituja*, which is consistent with their morphological similarities. Further investigation with precise species identification is needed to confirm the phylogenetic relationships within the family Stokesiidae.

Previous phylogenetic analyses of the genus *Frontonia*, type of Frontoniidae, suggested that *Frontonia* is paraphyletic, though these species share very similar morphological features (Strüder-Kypke et al., 2000; Gao et al., 2008; Fan et al. 2011, 2013; Pan et al. 2013). In our phylogenetic analyses, *Frontonia* species were further distributed across three clusters because *F. terricola* occupied a sister position to the family Stokesiidae, and was distant from the other two groups of the genus. However, there are no obvious morphological similarities between *F. terricola* and Stokesiidae (Foissner, 1987; Foissner et al., 1994). Sequencing and phylogenetic analyses were repeated but gave the same result. A possible explanation is that SSU rRNA genes are not good markers to reveal the phylogenetic relationships of frontoniids or the morphological similarities of frontoniids are due to congruent evolution.

Hypothetical systematic relationships of peniculid taxa based on both morphological and molecular data (Fig. 9; Table 3)

The order Peniculida includes six families after Maritujidae was synonymized. These families are Clathrostomatidae (Kahl, 1926), Frontoniidae (Kahl, 1926), Lembadionidae Jankowski in Corliss (1979), Neobursaridiidae Dragesco and Tuffrau, 1967,

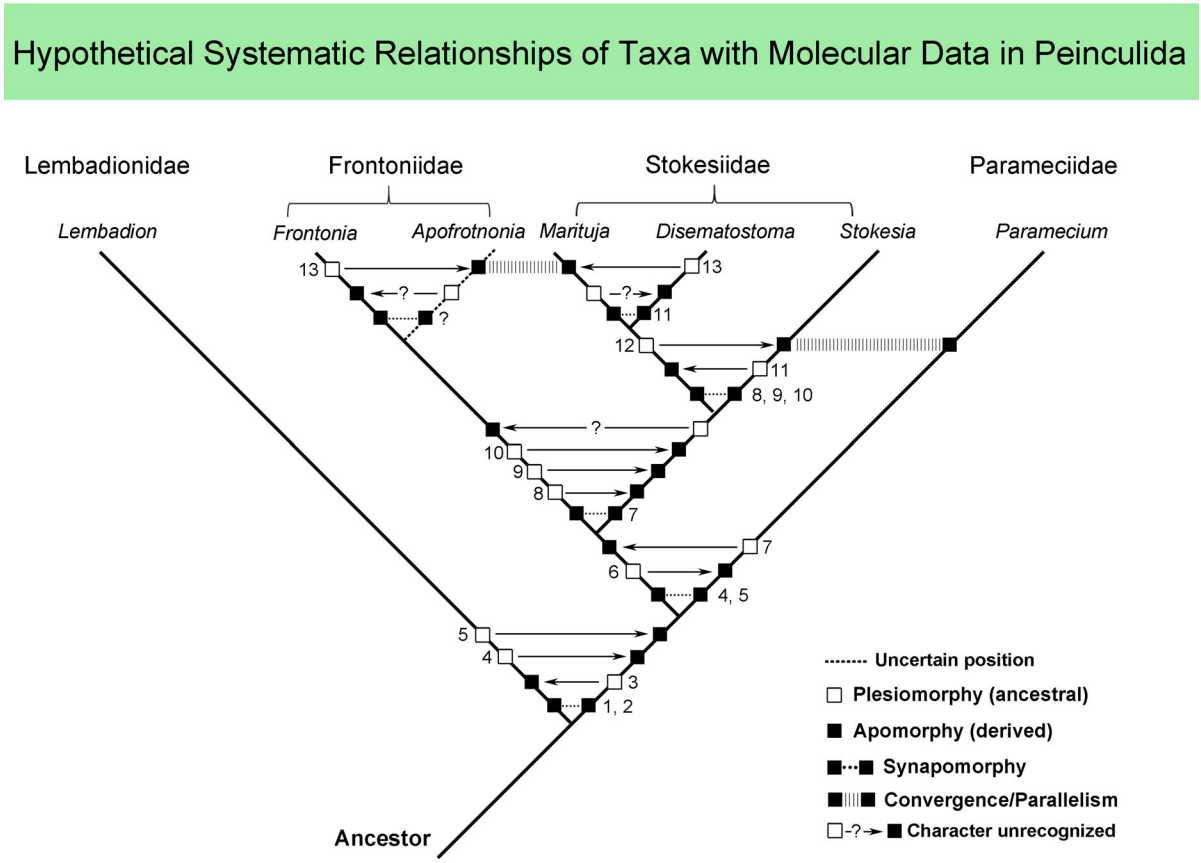

Fig. 9 Hypothetical systematic relationships of Peniculida taxa based on the combined phylogenetic analyses and morphological data. Character states used to separate taxa are listed in Table 3

Parameciidae Dujardin, 1840, and Stokesiidae Roque, 1961. Until now, SSU rRNA gene sequences were available for seven genera representing four of the six Peniculida families. As described and discussed above, the phylogenetic trees revealed some information regarding the relationships between some families of the order. Therefore, we propose a hypothesis of the systematic relationships of peniculids based on information from both molecular phylogeny and morphological references.

Peniculida is a well-defined monophyletic order, and all its members share at least two characteristics: somatic ciliature primarily containing dikinetids and buccal membranelles running parallel to the body long axis (Small & Lynn, 1985). Based on the phylogenetic position of Lembadionidae within this order, the feature "having an undifferentiated oral membranelle and associated fibers" (Guinea et al., 1990) may represent a plesiomorphic characteristic. The more complicated oral apparatus comprising three peniculi and developed associated oral microtubules, which is shared by Frontoniidae, Stokesiidae, and Parameciidae (Patterson, 1981; Small & Lynn, 1985; Gill, 1992), is likely a synapomorphy. According to Strüder-Kypke et al. (2000), the presence of trichocysts was a synapomorphy for peniculines, which was subsequently lost in Lembadionidae. We agree that possessing trichocysts represents an ancient feature, since the sister groups of peniculids, such as scuticociliates and hymenostomes, usually have certain kinds of extrusomes (Fan et al., 2010; Foissner, 2013).

In our phylogenetic analyses, Frontoniidae was distributed into three clades and most of its members were clustered with parameciids. However, the morphological data do not support their close relationship. Parameciidae possesses a prebuccal groove that is absent in all other members of Peniculida, including

Table 3 State of morphological characteristics assigned in the systematic relationships hypothesis in Fig. 9

□ Plesiomorph	■ Apomorph
1 Other	Somatic ciliature primarily containing dikinetids
2 Other	Oral membranelles parallel to body long axis
3 Trichocysts present	Trichocysts absent
4 Oral polykinetid undifferentiated, as single column	Oral polykenetid differentiated, as multiple columns
5 Associated microtubules of oral polykinetid undeveloped, as evenly distributed fine fibers	Associated microtubules of oral polykinetid developed
6 Prebuccal groove absent	Prebuccal groove present
7 Without vestibular kineties	Vestibular kineties present at right of the paroral membrane
8 Kinetids on dorsal side bearing cilia	Part of kinetids on dorsal side barren
9 Dorsal sutures as barren seem	Dorsal suture with ciliated kinetidal rows
10 Somatic ciliature only recognized as longitudinal rows	Somatic ciliature recognized also as transversely or obliquely oriented rows
11 Kinetidal rows of ciliated dorsal suture without developed associated fibers and is continuous with preoral suture	Kinetidal rows of ciliated dorsal suture (dorsal polar band) with developed fibers and connecting with postoral suture
12 Peniculus 3 composed of closely arranged kinetidal rows	Peniculus 3 composed of widely spaced kinetidal rows
13 Small vestibular cavity with few vestibular kineties	Larger vestibular cavity with increasing number of vestibular kineties

Lembadionidae, which represents a synapomorphy of the family. Similarly, vestibular kineties right of the paroral membrane possessed by both Frontoniidae and Stokesiidae can be a synapomorphy that derived from the ancestral status shown in Parameciidae and Lembadionidae (Didier, 1994; Strüder-Kypke et al., 2000).

Stokesiidae is a well-supported monophyletic family with synapomorphies including ciliated dorsal suture, barren kinetids on the dorsal side, and transversely oriented somatic ciliature. For the inner relationship of the three genera, we are inclined to consider *Marituja* as sister to *Disematostoma* as discussed above. Morphologically, the dorsal polar band in *Marituja* and *Disematostoma* is an apomorphic character compared to the ciliated dorsal suture of *Stokesia*, because its kinetidal rows are associated with developed fibers. On the contrary, the dorsal suture of *Stokesia* is more like normal somatic kineties, since no developed fibers have been reported to be associated with kinetosomes (Krainer, 1988, 1995; Foissner et al. 1999). Peniculus 3 of *Stokesia* includes widely arranged kinetidal rows, similar to the quadrulus (a peniculus 3 that is typically four kinetosomes in width and its lengthy rows are more loosely associated than is the case in other peniculi) of Parameciidae, which was reported as apomorphic (Wichterman, 1986). We agree with this viewpoint and speculate that the widely spaced rows of peniculus 3 are the result of convergent/parallel evolution between *Stokesia* and *Paramecium*.

Apofrontonia was classified into Frontoniidae when it was established (Foissner & Song, 2002), and it shares similar features with *Frontonia* in terms of body shape and ciliary pattern. These similarities include closely arranged kinetal rows in peniculi and vestibular kineties at right side of buccal opening. Fokin et al. (2006) considered *Apofrontonia* as a separate lineage, and assigned it as *incertae sedis* in Peniculida since it lacks oral nematodesmata, which is a typical feature of other frontoniids. Previous studies also noted that *Apofrontonia* was similar to *Marituja* based on the shape and large size of opening vestibule, and sausage-shaped macronucleus (Foissner & Song, 2002; Fokin et al., 2006). However, we noticed that it lacks the barren kinetids, dorsal polar band, and transversely oriented ciliature. Therefore, we accept the original classification assigning *Apofrontonia* in Frontoniidae for the time being, based on the close

relationship of *Apofrontonia* and *Frontonia* in the phylogenetic trees, despite that no synapomorphy has been identified yet. The similarities between *Apofrontonia* and *Marituja*, namely the large vestibule and increasing number of vestibular kineties, may be another case of convergent/parallel evolution.

The other two monotypic families, Clathrostomatidae and Neobursaridiidae, were not included in our hypothesis due to the lack of molecular information. Clathrostomatidae has slightly differentiated oral polykinetid as multiple dikinetid rows and nematodesmata around cytopharynx (Small & Lynn, 1985). We speculate that Clathrostomatidae is close to Frontoniidae and Stokesiidae, but occupies a more ancestral position. Neobursaridiidae is likely to be close to Parameciidae based on shared morphological features, such as having a complicated prebuccal groove and a peniculus 3 that contains widely separated kinetosome rows (Dragesco & Dragesco-Kernéïs, 1986; Lynn, 2008). There is a great need for expanded sampling for molecular data (more taxa and more marker genes), especially for these two families and the Frontoniidae, to provide a better understanding of the systematics in the order Peniculida.

Acknowledgements This work was supported by the National Natural Science Foundation of China [Nos. 31572223, 31601843], and the Fundamental Research Funds for the Central Universities (201762017). We thank Dr. Rui Ma and Dr. Bing Ni for their help with scanning electron microcopy.

References

Corliss, J. O., 1953. Silver impregnation of ciliated protozoa by the Chatton-Lwoff technic. Biotechnic and Histochemistry 28: 97–100.

Corliss, J. O., 1979. The Ciliated Protozoa. Characterization, Classification and Guide to the Literature. Pergamon Press, New York.

Didier, P., 1994. Sous-classe des Peniculia. In de Puytorac, P. (ed.), Infusoires ciliés. Fasc. 2. Systématique. Traité de Zoologie, Vol. 2. Masson Press, Paris: 603–620.

Dragesco, J. & D. Dragesco-Kernéïs, 1986. Cilies libres de l' Afrique intertropicale. Collection Faune Tropicale, Vol. 26. ORSTOM, Paris: 1–559.

Fan, X., X. Chen, W. Song, K. A. S. Al-Rasheid & A. Warren, 2010. Two new marine scuticociliates, *Sathrophilus planus* n. sp. and *Pseudoplatynematum dengi* n. sp., with improved definition of *Pseudoplatynematum* (Ciliophora, Oligohymenophorea). European Journal of Protistology 46: 212–220.

Fan, X., X. Chen, W. Song, K. A. S. Al-Rasheid & A. Warren, 2011. Two novel marine *Frontonia* species, *F. mengi* spec. nov. and *F. magna* spec. nov. (Protozoa; Ciliophora), with notes on their phylogeny based on SSU rRNA gene sequence data. International Journal of Systematic and Evolutionary Microbiology 61: 1476–1486.

Fan, X., X. Lin, W. Liu, Y. Xu, S. A. Al-Farraj & A. Warren, 2013. Morphology and phylogeny of three new marine *Frontonia* species (Ciliophora; Peniculida) from coastal waters of China. European Journal of Protistology 49: 312–323.

Foissner, W., 1987. Neue terrestrische und limnische Ciliaten (Protozoa, Ciliophora) aus Österreich und Deutschland. Sitzungsberichte der Akademie der Wissenschaften 195: 217–268.

Foissner, W., 2013. Description of *Glaucomides bromelicola* n. gen. n. sp. (Ciliophora, Tetrahymenida), a macrostome forming inhabitant of bromeliads (Bromeliaceae), including redescriptions of *Glaucoma scintillans* and *G. reniformis*. Journal of Eukaryotic Microbiology 60: 137–157.

Foissner, W. & W. Song, 2002. *Apofrontonia lametschwandtneri* nov. gen., nov. spec., a new peniculine ciliate (Protozoa, Ciliophora) from Venezuela. European Journal of Protistology 38: 223–234.

Foissner, W., H. Berger & F. Kohmann, 1994. Taxonomische und ökologische Revision der Ciliaten des Saprobiensystems-Band III: Hymenostomata, Prostomatida, Nassulida. Informationsberichte des Bayerrischen Landesamtes für Wasserwirtschaft 1(94): 1–548.

Foissner, W., H. Berger & J. Schaumburg, 1999. Identification and ecology of limnetic plankton ciliates. Informationsberichte des Bayerrischen Landesamtes für Wasserwirtschaft 3(99): 1–793.

Fokin, S. I., 2008. Rediscovery and characterization of *Frontonia fusca* (Quennerstedt, 1869) Kahl, 1931 (Ciliophora, Peniculia). Denisia 23: 251–259.

Fokin, S. I., I. Andreoli, F. Verni & G. Petroni, 2006. *Apofrontonia dohrni* sp. n. and the phylogenetic relationships within Peniculia (Protista, Ciliophora, Oligohymenophorea). Zoologica Scripta 35: 289–300.

Gao, S., Z. Chen, C. Shao, H. Long, K. A. S. Al-Rasheid & W. Song, 2008. Reconsideration of the phylogenetic position of *Frontonia*-related Peniculia (Ciliophora, Protozoa) inferred from the small subunit ribosomal RNA gene sequences. Acta Protozoologica 47: 47–54.

Gao, F., A. Warren, Q. Zhang, J. Gong, M. Miao, P. Sun, D. Xu, J. Huang, Z. Yi & W. Song, 2016. The all-data-based evolutionary hypothesis of ciliated protists with a revised classification of the phylum Ciliophora (Eukaryota, Alveolata). Scientific Reports 6: 24874.

Gill, R., 1992. Cytoskeletal elements of *Frontonia leucas* (Ciliophora: Hymenostomatida). Transactions of the American Microscopical Society 111: 327–337.

Gouy, M., S. Guindon & O. Gascuel, 2010. SeaView version 4: a multiplatform graphical user interface for sequence alignment and phylogenetic tree building. Molecular Biology and Evolution 27: 221–224.

Gu, F. & B. Ni, 1993. The exploration of preparing protozoan specimen for scanning electron microscopy. Journal of Chinese Electron Microscopy Society 12: 525–529.

Guinea, A., A. Sola, J. Longas & D. Fernandez-Galiano, 1990. Morphology and morphogenesis of two species of the genus *Lembadion* (Ciliophora, Oligohymenophora): *Lembadion lucens* and *Lembadion bullinum*. Journal of Eukaryotic Microbiology 37: 553–561.

Huang, J., Z. Chen, W. Song & H. Berger, 2014. Three-gene based phylogeny of the Urostyloidea (Protista, Ciliophora, Hypotricha), with notes on classification of some core taxa. Molecular Phylogenetics and Evolution 70: 337–347.

International Commission on Zoological Nomenclature, 1999. International code of zoological nomenclature, adopted by the International Union of Biological Sciences. International Trust for Zoological Nomenclature, London.

Jankowski, A. W., 2007. Phylum Ciliophora Doflein, 1901. In Alimov, A. F. (ed.), Protista. Part 2, Handbook on Zoology. Russian Academy of Sciences, Zoological Institute, Nauka, St. Petersburg: 415–993.

Kahl, A., 1926. Neue und wenig bekannte Formen der holotrichen und heterostrichen Ciliaten. Archiv Für Protistenkunde 55: 197–438.

Kahl, A., 1931. Urtiere oder Protozoa I: Wimpertiere oder Ciliata (Infusoria). 2. Holotricha. Tierwelt Dtl 21: 181–398.

Krainer, K. H., 1988. Alpha-Taxonomie und Ökologie neuer sowie mehrerer wenig bekannter pelagischer Ciliaten (Protozoa: Ciliophora aus den Klassen Kinetofragminophora, Oligohymenophora, Polyhymenophora) einiger Grundwasserbaggerteiche des nordlichen Leibnitzer Feldes (Steiermark, Österreich). Dissertation of University of Graz, 209+41.

Krainer, K. H., 1995. Taxonomische Untersuchungen an neuen und wenig bekannten planktischen Ciliaten (Protozoa: Ciliophora) aus Baggerseen in Österreich. Lauterbornia 21: 39–68.

Krenek, S., T. U. Berendonk & S. I. Fokin, 2015. New *Paramecium* (Ciliophora, Oligohymenophorea) congeners shape our view on its biodiversity. Organisms Diversity & Evolution 15: 215–233.

Long, H., W. Song, J. Gong, X. Hu, H. Ma, M. Zhu & M. Wang, 2005. *Frontonia lynni* n. sp., a new marine ciliate (Protozoa, Ciliophora, Hymenostomatida) from Qingdao, China. Zootaxa 1003: 57–64.

Long, H., W. Song, K. A. S. Al-Rasheid, Y. Wang, Z. Yi, S. A. Al-Quraishy, X. Lin & S. A. Al-Farraj, 2008. Taxonomic studies on three marine species of *Frontonia* from northern China: *F. didieri* n. sp., *F. multinucleata* n. sp. and *F. tchibisovae* Burkovsky, 1970 (Ciliophora: Peniculida). Zootaxa 1687: 35–50.

Lynn, D. H., 2008. The Ciliated Protozoa. Characterization, Classification, and Guide to the Literature. Springer, Dordrecht.

Ma, H., J. K. Choi & W. Song, 2003. An improved silver carbonate impregnation for marine ciliated protozoa. Acta Protozoologica 42: 161–164.

Martin-Gonzaleaz, A., S. Serrano & D. Fernandez-Gallano, 1990. On the morphology, morphogenesis, and argyrome of *Dissematostoma buetschlii* (Ciliophora, Frontoniidae). Canadian Journal of Zoology 68: 245–253.

Medlin, L., H. J. Elwood, S. Stickel & M. L. Sogin, 1988. The characterization of enzymatically amplified eukaryotic 16S-like rRNA-coding regions. Gene 71: 491–499.

Michiels, M. & N. Wilbert, 1973. Etude morphologique du cilié hyménostome péniculien *Disematostoma minor* Kahl, 1926. Protistologica 4: 455–458.

Miller, M. A., W. Pfeiffer & T. Schwartz, 2010. Creating the CIPRES Science Gateway for inference of large phylogenetic trees. Gateway Computing Environments Workshop 14: 1–8.

Nylander, J. A., 2004. MrModeltest v2. Uppsala University, Uppsala.

Obolkina, L. A., 1995. Ciliophora. In Timoshkin, O. A. (ed.), Guide and Key to Pelagic Animals of Baikal with Ecological Notes. "Nauka" Siberian Publishing Firm RAS, Novosibirsk: 182–205.

Packroff, G. & N. Wilbert, 1991. Taxonomische studien über die ciliatenfauna (Protozoa, Ciliophora) der Eifelmaare. Archiv Für Protistenkunde 140: 121–139.

Pan, X., W. Liu, Z. Yi, X. Fan, K. A. S. Al-Rasheid & X. Lin, 2013. Studies on three diverse *Frontonia* species (Ciliophora, Peniculida), with brief notes on 14 marine or brackish congeners. Acta Protozoologica 52: 35–49.

Patterson, D. J., 1981. On the origin of the postoral microtubules of *Paramecium putrinum* (Hymenostomatida, Ciliophora). Protistologica 4: 525–531.

Penn, O., E. Privman, H. Ashkenazy, G. Landan, D. Graur & T. Pupko, 2010a. GUIDANCE: a web server for assessing alignment confidence scores. Nucleic Acids Research 38: W23–W28.

Penn, O., E. Privman, G. Landan, D. Graur & T. Pupko, 2010b. An alignment confidence score capturing robustness to guide tree uncertainty. Molecular Biology and Evolution 27: 1759–1767.

Posada, D. & K. A. Crandall, 1998. Modeltest: testing the model of DNA substitution. Bioinformatics 14: 817–818.

Ronquist, F. & J. P. Huelsenbeck, 2003. MRBAYES 3: Bayesian phylogenetic inference under mixed models. Bioinformatics 19: 1572–1574.

Serrano, S., A. Sola, A. Guinea & R. Gil, 1990. Morphology and morphogenesis of *Disematostoma colpidioides* (Ciliophora, Frontoniidae): its systematic implications. European Journal of Protistology 25: 353–360.

Serrano, S., R. Gil, A. Sola, L. Arregui & A. Guinea, 1994. Cytoskeletal organization of *Disematostoma colpidioides* (Ciliophora, Frontoniidae). Acta Protozoologica 33: 87–92.

Small, E. B. & D. H. Lynn, 1985. Phylum Ciliophora, Doflein, 1901. In Lee, J. J., S. H. Hutner & E. C. Bovee (eds), An Illustrated Guide to the Protozoa. Society of Protozoologists, Lawrence: 393–575.

Stamatakis, A., 2014. RAxML Version 8: A tool for phylogenetic analysis and post-analysis of large phylogenies. Bioinformatics 30: 1312–1313.

Strüder-Kypke, M. C., A. D. Wright, S. I. Fokin & D. H. Lynn, 2000. Phylogenetic relationships of the subclass Peniculia (Oligohymenophorea, Ciliophora) inferred from small subunit rRNA gene sequences. Journal of Eukaryotic Microbiology 47: 419–429.

Suzuki, T. & C. Miyabe, 2007. Ecological balance between ciliate plankton and its prey candidates, pico- and nanoplankton, in the East China Sea. Hydrobiologia 586: 403–410.

Tarcz, S., 2013. Intraspecific differentiation of *Paramecium novaurelia* strains (Ciliophora, Protozoa) inferred from phylogenetic analysis of ribosomal and mitochondrial DNA variation. European Journal of Protistology 49: 50–61.

Tuffrau, M. & A. Savoie, 1961. Etude Morphologique du Cilié Hymenostome *Disematostoma colpidioides* von Gelei, 1954. The Journal of Protozoology. 8: 64–68.

Warren, A., D. J. Patterson, M. Dunthorn, J. C. Clamp, U. E. Achilles-Day, E. Aescht, S. A. Al-Farraj, S. Al-Quraishy, K. Al-Rasheid, M. Carr, J. G. Day, M. Dellinger, H. A. El-Serehy, Y. Fan, Y. Fan, Y. Fan, F. Gao, S. Gao, J. Gong, R. Gupta, X. Hu, K. Kamra, G. Langlois, X. Lin, D. Lipscomb, C. S. Lobban, P. Luporini, D. H. Lynn, D. H. Lynn, D. H. Lynn, H. Ma, M. Macek, J. Mackenzie-Dodds, S. Makhija, R. I. Mansergh, M. Martín-Cereceda, N. McMiller, D. J. S. Montagnes, S. Nikolaeva, G. O. Ong'ondo, B. Pérez-Uz, J. Purushothaman, P. Quintela-Alonso, J. Rotterová, L. Santoferrara, C. Shao, Z. Shen, X. Shi, W. Song, T. Stoeck, A. La Terza, A. Vallesi, M. Wang, T. Weisse, K. Wiackowski, L. Wu, K. Xu, Z. Yi, R. Zufall & S. Agatha, 2017. Beyond the "Code": a guide to the description and documentation of biodiversity in Ciliated Protists (Alveolata, Ciliophora). Journal of Eukaryotic Microbiology. doi:10.1111/jeu.12391.

Wichterman, R., 1986. The Biology of Paramecium. Plenum, New York.

Wiackowski, K. & W. Kocerba-Soroka, 2017. Selective predation by a harpacticoid copepod on ciliates in phytotelmata: a laboratory experiment. Hydrobiologia 790: 13–22.

Wilbert, N., 1972. Die Infraciliatur von *Marituja pelagica* Gajewskaja, 1928. The Journal of Protozoology 19: 590–592.

Wilbert, N., 1975. Eine verbesserte Technik der Protargolimprägnation für Ciliaten. Mikrokosmos 64: 171–179.

Yildiz, I. & N. G. Senler, 2013. *Frontonia anatolica* n. sp. a new peniculid ciliate (Protista, Ciliophora) from Lake Van, Turkey. Turkish Journal of Zoology 37: 24–30.

Zhao, Y., E. Gentekaki, Z. Yi & X. Lin, 2013. Genetic differentiation of the mitochondrial cytochrome oxidase *c* subunit I gene in genus *Paramecium* (Protista, Ciliophora). Plos ONE 8: e77044–e77044.

Zhao, Y., Z. Yi, E. Gentekaki, A. Zhan, S. A. Al-Farraj & W. Song, 2016. Utility of combining morphological characters, nuclear and mitochondrial genes: an attempt to resolve the conflicts of species identification for ciliated protists. Molecular Phylogenetics and Evolution 94(Pt B): 718–729.